CRM content of bottom ash treatment material streams

TNO Public ⟩ TNO 2025 R16290
30 March 2026

Netherlands Materials Observatory
www.nederlandsmaterialenobservatorium.nl/en/
+31 88 866 43 00
info@nederlandsmaterialenobservatorium.nl

TNO 2025 R16290 – 30 March 2026

Authors	Douwe Huitema, Susanne van Berkum, Soroush Aghaeian
Reviewers	Ton Bastein, Joris Dijkstra, Patrick Aerts
Report classification	TNO Public
Page numbers	30 (excl. back cover)
Number of attachments	1

Executive summary

This case study explores the potential for recovering critical raw materials (CRMs) from bottom ash treatment in the Netherlands. Although earlier studies have quantified CRM presence in raw incinerator bottom ash (IBA), little is known about the CRM concentrations in the separate processed Incinerator Bottom Ash Aggregate (IBAA) and other material streams produced by bottom ash recyclers. Given that bottom ash treatment facilities produce more than 20 distinct material fractions through complex mechanical and chemical processes, this knowledge gap limits the ability to assess the feasibility of CRM recovery.
At the Heros facility in Sluiskil the Netherlands, roughly one million tonnes of IBA are treated annually using a sequence of mechanical separation technologies and washing technologies. This process already yields over 100,000 tonnes of ferrous metal per year, contributing to national circular economy objectives.

To assess CRM presence in the separate output material streams, a selection of samples from the process were analysed by ICP-MS. Results show significant concentrations of elements such as Cu, Ni, Al, Sr, Mn, Mg, Ti and B. The range of measured concentrations is fairly homogeneous for the different samples, disproving our hypothesis that CRMs would ‘pile up’ in certain material streams because of the array of sorting techniques. However, several samples displayed concentrations comparable to average global ore grades for Co, Cu and Sr. These findings indicate that certain bottom ash treatment outputs may have potential as secondary CRM sources.

Nevertheless, the dataset is limited to one ICP-MS measurement per sample. The results require validation through additional measurements, including sampling and analysis of coarse fractions, before statements on CRM concentrations can confidently be proved or disproved. Once CRM concentrations have been confirmed by multiple measurements, follow up hydrometallurgy experiments on the actual recovery of critical elements could be performed. Additionally, broader studies across different ash sources (from other Dutch bottom ash or other EU countries) could reveal additional sources for CRMs.

Contents

1 Introduction

1.1 Netherlands Materials Observatory

The Netherlands Materials Observatory (NMO) collects, manages, and provides data, information, and knowledge about the presence and supply chains of critical raw materials (CRMs) strategic raw materials (SRMs), as defined by the EU Critical Raw Material Act (CRMA). In doing so, the NMO contributes to a resilient and robust economy and society. The NMO works together with the Dutch national government, companies and research institutions in the Netherlands and abroad. The NMO provides insight into the supply and availability of these critical raw materials in the Netherlands and the European Union (EU). An enhanced understanding enables policymakers and businesses to better respond to risks associated with supply chain disruptions.

As a part of this overarching task, the NMO works with partners from the recycling value chain and the research community to analyse how the Netherlands (and neighbouring countries) can contribute towards increasing recycling contributions and, by extension, the Critical Raw Mate-rial Act benchmarks.

Therefore, the NMO conducts case studies to understand the context and background of different Dutch waste streams, end-of-life of product groups, and secondary materials. These case studies provide relevant information about CRMs present in such materials and waste streams and discuss potential recovery pathways and challenges for such CRMs.

1.2 Bottom ash treatment products as a source for CRMs

This case study focuses on the material streams that result from bottom ash (bottom ash is the ash remaining from incineration of household waste) treatment. The Dutch National Exploration Programme (TNO, 2025) has already mapped the potential of bottom ash as a source for critical raw materials. In short: *bottom ash contains a large variety of CRMs, the volume is enormous and in the state of the art, only common and or payable resources such as iron, copper, platinum and aggregates are recovered.*

Many existing scientific papers have already mapped the CRM content of raw bottom ash, including specific studies on Dutch bottom ash by Dijkstra (Dijkstra, 2019). The theoretical potential from an input perspective is apparent, but CRMs are not easily recovered from raw bottom ash. Bottom ash recyclers exploit an intricate series of recycling technologies, producing more than 20 material streams in the process. And contrary to the studies on raw bottom ash, no literature is available on the CRM concentrations of these material streams. Our hypothesis is that CRM concentrations will differ significantly for the different material streams that result from bottom ash treatment processes. By identifying the material streams where CRMs pile up, we can present opportunities for bridging the gap between the theoretical CRM potential and the Dutch practice of bottom ash treatment.

This report gives a first indication on this hypothesis, through documenting the results of a sampling and mass spectral analysis done at the Heros bottom ash treatment facility. After a brief description of the bottom ash context in chapter 2, the bottom ash treatment process is described in chapter 3 and the experimental method in chapter 4. The results from the exploratory study are shown in chapter 5, followed by a conclusion in chapter 6.

2 Bottom Ash Context

2.1 What is bottom ash?

Incineration bottom ash (IBA) is the raw heavy, heterogeneous solid ash residue that remains on the combustion grate of municipal solid waste incinerators (MSWI) after incinerating municipal waste. It consists of inert, non-combustible materials such as sand and stones, as well as metals and fragments of residual waste that were not completely incinerated. Fresh IBA is basic, with a pH value of 10.5 – 12. Its particle size distribution is heterogeneous: 30 – 40 % is smaller than 2 mm, and 20% is larger than 2 cm (Šyc et al., 2020).

Figure 1 shows Dutch bottom ash after incineration. Bottom ash treatment companies can clearly distinguish between Dutch and foreign bottom ash based on colour and texture. Dutch MSWI focuses on energy generation, treating waste as a fuel that must burn efficiently but not completely. This is reflected in the bottom ash, which contains more non-incinerated waste compared to, for example, French bottom ash, which results from a more complete incineration process (e.g., longer). Bottom ash should not be confused with fly ash, which is collected from the air emission control systems of MSWI.

Figure 1 Close up photo of Dutch bottom ash (picture by TNO)

2.2 Elemental composition

The elemental composition of IBA has been studied on several occasions in literature, both from the perspective of toxic elements and of IBA as a critical resource. Table 1 shows combined results from literature, where CRMs and SRMs are highlighted in orange. Some significant concentrations are found for Al, Cu, Mg, Mn, Ni and P, but less common elements like Nb, Sc and Sm show presence as well.

	Elemental composition mg/kg				
Element	Dijkstra 2019 *Dutch average*	Hjelmar 2013 *EU average*	Funari 2015 *Italian*	Astrup 2016 *Worldwide*	Ghani 2023 *Italian*
Ag		15.2			
Al	40000	47232		14000-79000	
As		17.3	9.4	0.012-190	11.1
B		198			
Ba		1102	1122	69-57000	915
Be		1.2			
Bi		2.1			
Br		44.7			
C		3171			
Ca	87000	130833		8600-170000	
Cd		4.8		3-70	
Ce		0	23.7		22.5
Cl	4000	9211			
Co		31.8	22.7		52.3
Cr	500	353	606	20-3400	192
Cu	3000	3275	2459	190-25000	2395
Ga		0	9.4		
F		148			
Fe	92000	58714		3100-150000	
Hg		2.3			
K	9000	7748		660-16000	
La		0	14.1		12
Mg	13000	12429		240-26000	
Mn	1000	1173		0.77-3200	
Mo		30.1	15.2	0.25-280	9.1
Na	21000	21379		2200-42000	
Nb		0	12.4		
Nd		0	8.7		9.2
Ni		185	163	0.7-4300	99.8
P	3000	5633		440-10500	
Pb	3000	1309	354	7.4-14000	941
Rb		0	25.5		
S	8000	3862			
Sb		73			
Se		5.2		0.05-1	
Si	216000	82713		4300-308000	
Sc		0	14.3		2.45
Sm		0	1.8		1.95
Sn		181	358	0.3-470	
Sr		271	356		402
Ti	6000	6.7		0.008-0.23	
V	500	41.2	132		
Y		0	15		8.65
Zn	4000	3241	3443	1-20000	5395
Zr		0	165		

Table 1: The reported elemental compositions of industrial bottom ash from various scientific sources for the different bottom ash sample origins. CRMs have been marked in orange. A blank space indicates that a scientific source has not measured a particular elemental composition.

2.3 Economics

The European economics of bottom ash recycling have been addressed in the State of Play NMO study (TNO, 2026). Trade data show that the Netherlands imports some bottom ash from neighboring countries for processing, given the country's specialized facilities. The resulting ferrous and non-ferrous material streams are then exported again to smelters. Environmental concerns currently halt the domestic use of the aggregates that are recovered from treatment, even though part of the materials is compliant with soil quality policies. As a result, the aggregates pile up at washers or are exported.

3 Bottom ash treatment process

Given the heterogenous and coarse nature of bottom ash, the material requires further processing to recover valuable materials and produce secondary raw materials suitable for construction applications. Heros Sluiskil is the largest of 3 Dutch bottom ash treaters and processes approximately 1,000,000 tons of raw IBA annually from the Netherlands, Belgium and France. In comparison: this is more than half of the Dutch annual production of 1.7 Mt and accounts for the waste of roughly 10 million citizens. The goal of bottom ash treatment is to recover metals and produce certified aggregate fractions for use as circular building materials. The facility of Heros yields over 100,000 tons of ferrous scrap annually, supplying purified metal fractions to steel mills in the Netherlands and internationally.

The HEROS bottom ash treatment process is characterized as a dry treatment process and involves a complex sequence of several recycling technologies: drying, mechanical separation, wind shifting, crushing, sieving, magnetic separation, eddy current separation and finally washing. The other Dutch bottom ash treaters HVC and ACCN exploit a wet treatment process, where ashes are sorted in wet state.

Figure 2 shows pictures of typical materials resulting from the Heros treatment process. Figure 3 shows the flowchart of the simplified process at Heros for the mechanical separation processes pretreatment in CBOI 2010 and the mechanical sorting in CBOI 2017. Figure 4 depicts a first washing for minerals at WASI 1 and Figure 5 shows the second washing for concentrates and magnetic slag at WASI 2.

The next paragraph will describe the individual recycling steps of these parts. Sampled material fractions are marked in bold orange.

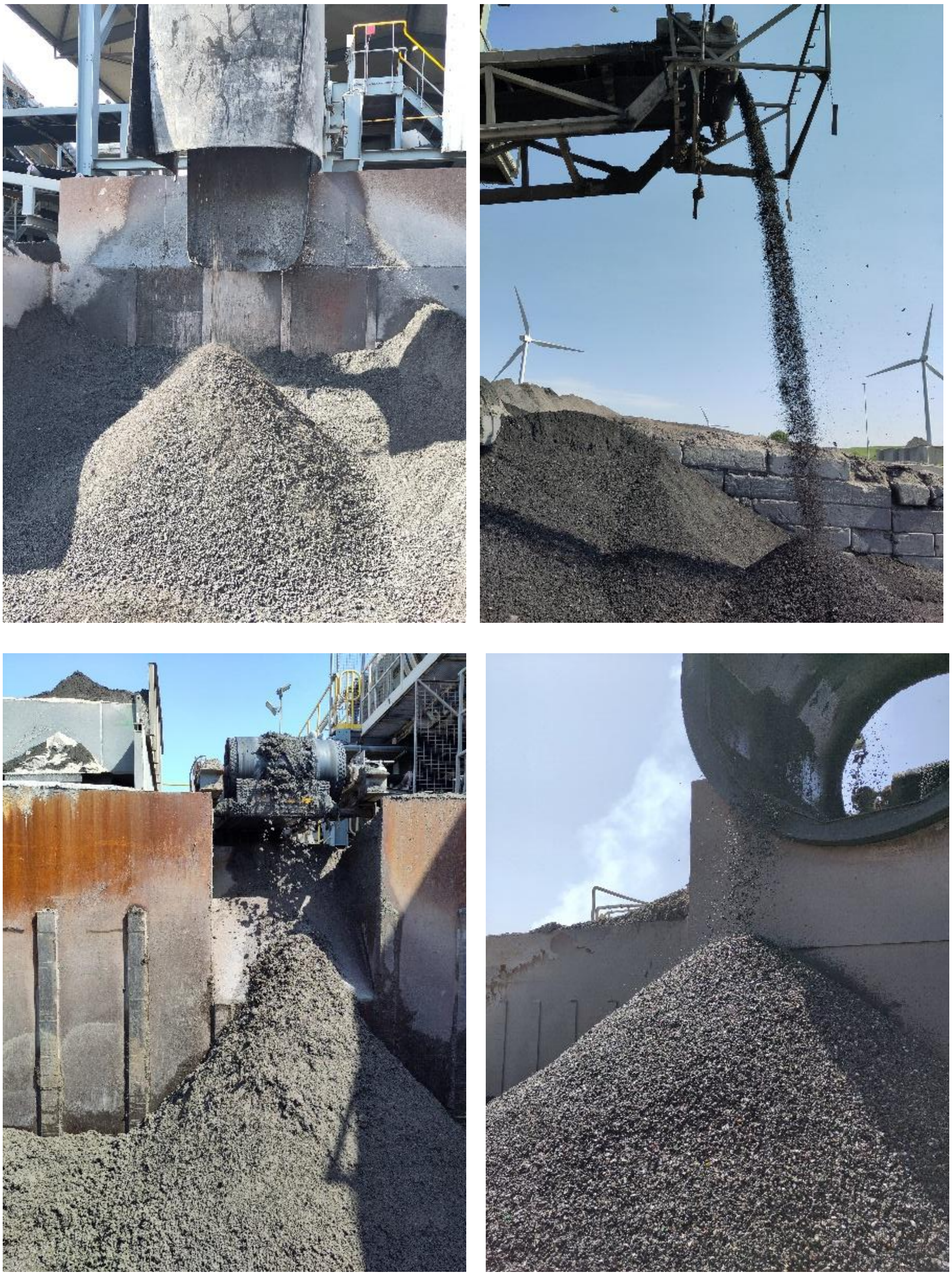

Figure 2: A photo impression of recycling steps at Heros. In clockwise rotation: ferrous slag recovery (sample W), the medium fine bottom ash output (sample X), washed sand (sample P) and coarse washed concentrate (sample U)

3.1 CBOI 2010 – pretreatment

The first pretreatment stage has the primary bottom ash as input material and involves the following steps:
Separation 1A: Ferrous fractions are separated through several steps of magnetic separation. Removal of coarse fractions that were not incinerated, along with wood, stone, and light materials (fluff) occurs via sieving and wind shifters.

Separation 1B: At this stage, magnetic slag from the crusher is added for further crushing. After crushing, large ferrous metals (Fe 40+ mm), non-ferrous metals (NF 40+ mm), and oversized mineral fractions (debris 40+ mm) are separated via *sieves*. The remaining finer fraction of bottom ash aggregate (IBAA 0-40 mm) together with the fine ferrous fraction are moved to the next steps of the CBOI 2010 pretreatment, which focus on finer separations (steps 2A and 2B):

Separation 2A: Recovery of ferrous metals and magnetic slag via magnetic separation.

Separation 2B: Fluff is removed via wind shifters. Several rounds of sieving and magnetic separation, separate non-ferrous metals in the 2–40 mm range (e.g. aluminium, copper, fractions F, G, H, I, J, K, L), very fine aggregate (IBAA 0-2 mm. Y, Z) and oversized aggregate (IBAA 40+ mm) bottom ash, and magnetic slag from crusher (fraction AA).

3.2 CBOI 2017 – finer mechanical separation

The remaining bottom ash aggregate (IBAA 2-40 mm) goes through the next step (CBOI 2017) for further refinement:
Separation 3A (with crusher): Additional magnetic slag is added and crushed with the rest of the material stream. IBAA 20+ mm is sieved out. Fluff and stainless steel (RVS) are separated via windshifters.

Separation 3B: Separation of non-ferrous metals in the 2–18 mm range via eddy-current units. Two size ranges of bottom ash aggregates - IBAA 0–2 mm (fraction V), IBAA 2–14 mm (fraction X) - are separated with sieves. The magnetic slag from breaker (fraction W) is separated via magnets.

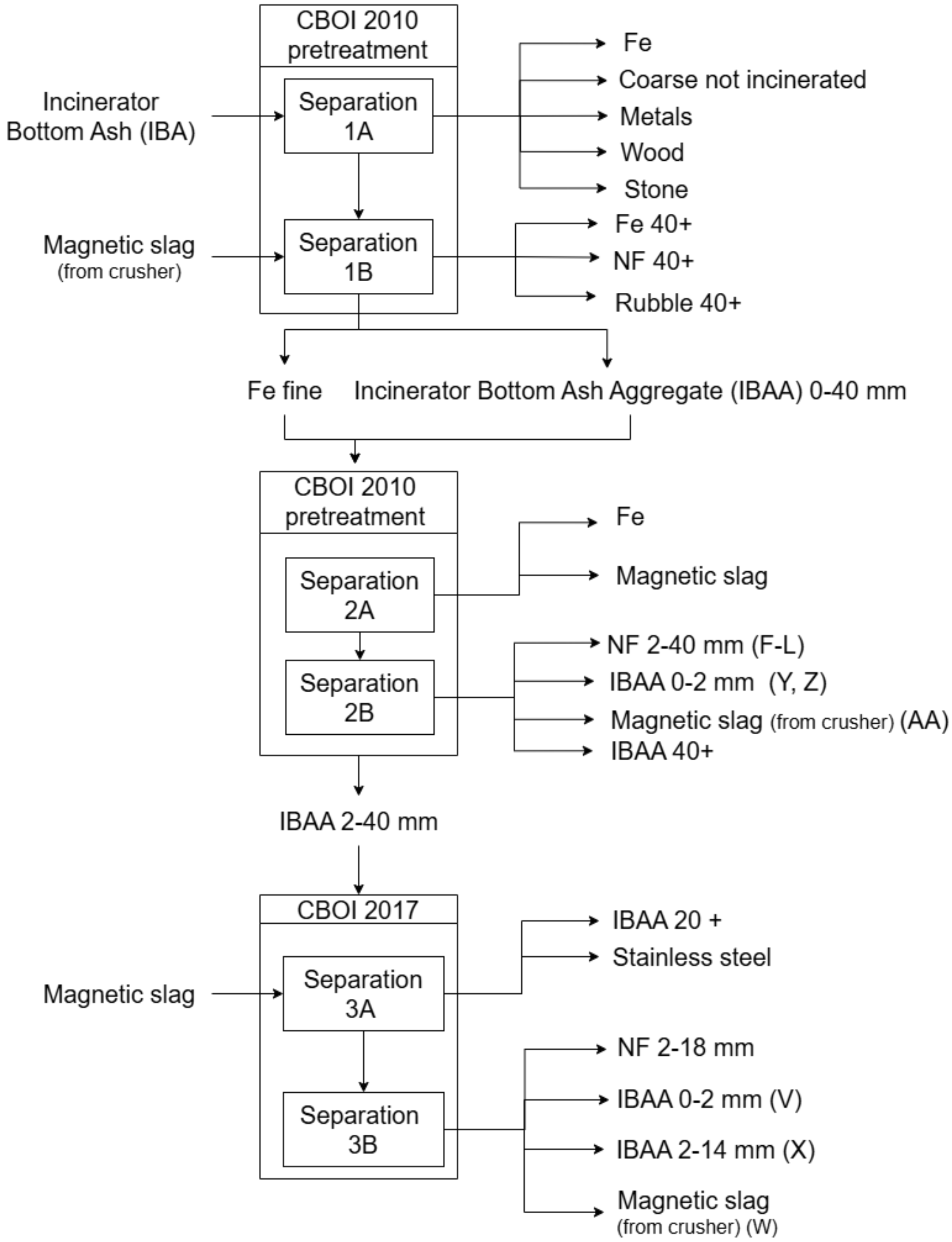

Figure 3: Simplified process flow diagram for mechanical separation processes for bottom ash treatment.

3.3 WASI 1 – first washing

After dry processing, bottom ash undergoes washing to remove salts, fine contaminants, and organic residues. The first washing process includes:
Washing step 1A: Initial washing of aggregate fractions (IBAA 0–2 mm and 2–14 mm), organic gravel and fluff.

Separation 4A: Separation of gravels (0.063–14 mm) (AB, O).

Washing step 1B: Separation of sand particles (0.063–2 mm) (AF).

Then the material goes through the settling stages:
Pre-settler: Primary settling for silt water (B).

Settler: Secondary settling for silt (A) and floating layers (AE).

Tank: Final clarification, producing effluent (C) and silt cake (AD).

Finally, **Separation 4C** removes remaining organic material (AC) and fluff.

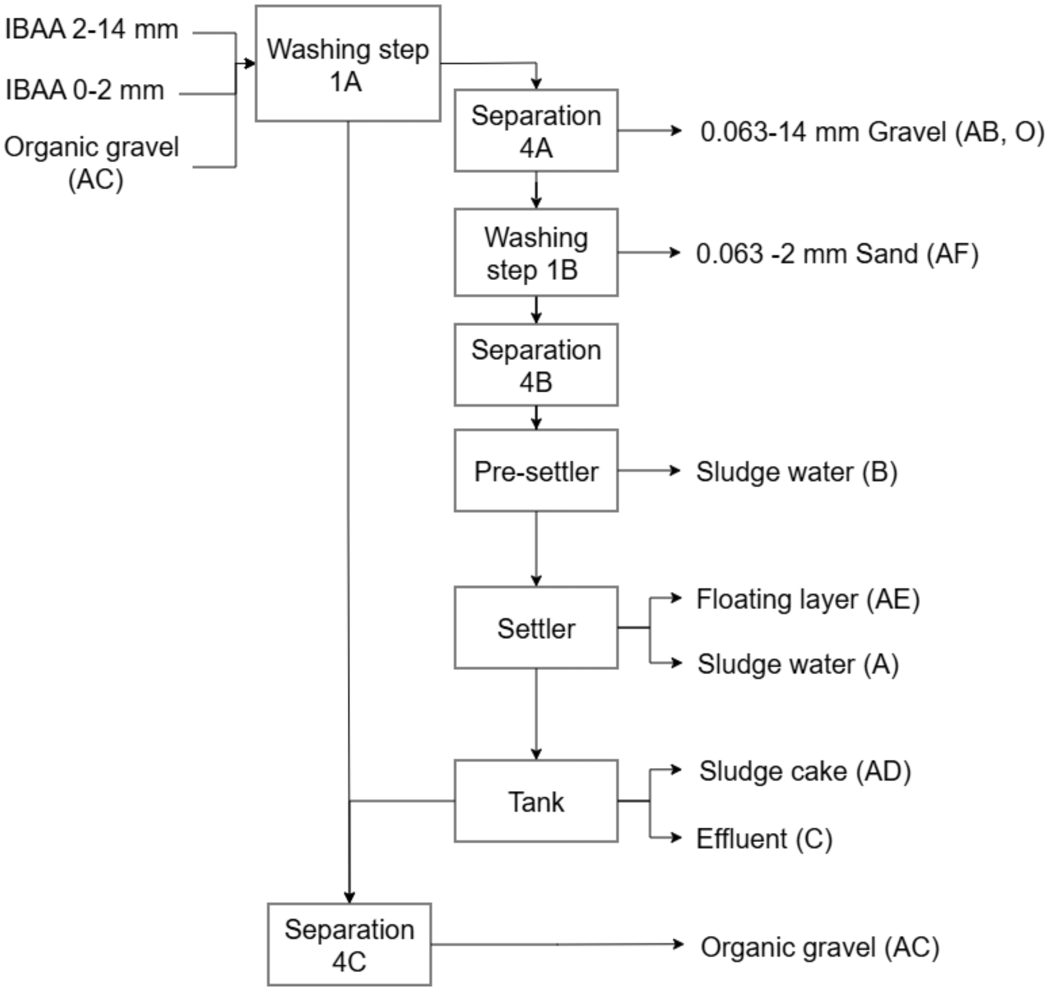

Figure 4: Simplified process flow diagram for first washing of bottom ash.

3.4 WASI 2 – second washing

After the initial washing stage, the fraction IBAA 0–14 mm (T) undergoes a second washing process to further clean and classify the material. This stage focuses on removing remaining contaminants and recovering valuable mineral fractions.
Washing step 2A: The material is washed to remove organic fluff and soil (Q). This step improves the environmental quality of the bottom ash by reducing organic content.

Separation 5A: The washed material is screened to separate fine and coarse fractions for subsequent processing.

Separation 5B: A density-based separation process that isolates mineral fractions from lighter contaminants. The output includes IBAA 0.063–14 mm washed aggregate fraction (P, U), which is suitable for use as a secondary raw material.

Separation 5C: Magnetic separation combined with screening removes remaining magnetic slag (M) and oversized particles (S).

Separation 5D and 5E: These steps refine the coarse (R) and fine concentrate (N) respectively.

Finally process water (D) and silt water (E) are collected for treatment in the wastewater system. This wastewater is treated on-site in a biological wastewater treatment plant. This facility consists of several procedures: acceptance, testing, storage, processing, and discharge of treated water, ensuring compliance with environmental regulations.

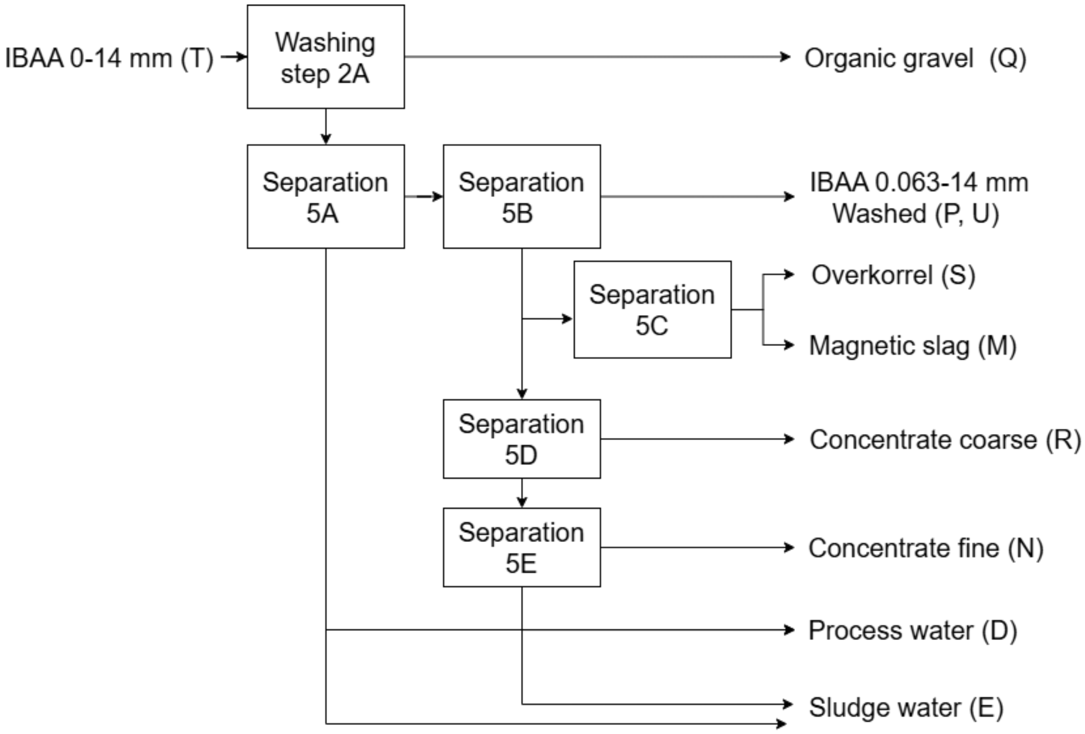

Figure 5: Simplified process flow diagram for second washing step of bottom ash.

4 Sampling and analysis methods

4.1 Sample origin

Samples were taken by operators at the site of Heros during treatment of a batch of raw bottom ash from a single site processing municipal household waste in the Netherlands. Samples were taken every two hours (approximately four samples per shift) from different output material streams as well as in-line samples as indicated in the process flow diagrams with a capital letter in between parentheses, e.g. (A). Samples were collected over time in large containers until the complete batch was processed. The duration of the campaign was 10 working days covering 20 shifts.

4.2 Solid samples

Sample preparation by Heros took place at the Heros laboratory and consisted of taking a representative sample using a splitter. Samples mainly consisting of sand-like materials were dried and milled using a jaw breaker or crusher when necessary. This was followed by several separation steps. Each of the separated material streams were collected and weighed. The results can be found in Table 6 of the Supplement chapter. Coarse metallic particles were removed by sieving and the remaining materials were further milled to be suitable for analysis. The same principle was performed for samples from outputs mainly recovering non-ferrous materials. These were dried and coarse non-ferrous materials were separated using a lab-sized Eddy current separator.

In total 90 bottom ash samples ranging from 0.1 to 3kg were received in sealed bags. 63 samples contained materials as obtained directly from the process and 27 samples contained materials that were further milled at the Heros laboratory. These 27 samples were taken for analysis at the TNO laboratory. Analysis was performed on dry samples, however the data reported here is not corrected for the dry weight. Typically, the original samples would contain 4-25 wt% of moisture.

The supplementary information reports on the removed coarse ferrous and non-ferrous fractions of the samples, which have not been analysed because they were too bulky for milling.

4.3 Liquid samples

Liquid samples did not undergo any further preparation before sending to TNO. At TNO, the five 10-L jerrycans of liquids were homogenized by pouring the contents between the jerrycan and a large beaker three times. A 50 mL subsample was taken, centrifuged (Hermle Z383K, 2500 rpm, 5 min), and the liquid was filtered through a 0.45 µm PES membrane. A portion of 8 mL was digested with HNO_3 for ICP-QQQ analysis.

The solid centrifugation residue was dried at 40 °C for 48 h, after which 0.1 g was subsampled for digestion. Liquid and solid results were later combined to reconstruct the original sample composition. The percentage of filtered dry weight in comparison to the total sample is given in the Supplement.

4.4 ICP-MS analysis

The milled fraction from one Dutch bottom ash batch was measured using inductively coupled plasma mass spectrometry (ICP-MS). All solid samples, including residues from the liquid samples were digested following SOP AC-W-037 (open DigiPrep digestion), a method developed by TNO. For each sample:

1. 0.1 g of powdered material was weighed into a digestion vessel.
2. 20 mL of acid mixture was added (16 mL 69% HNO_3 + 4 mL 30% H_2O_2).
3. Digestion was performed using a DigiPrep block at 106 °C for 120 min.
4. After digestion, samples were diluted to 50 mL with ultrapure water (final ~32% HNO_3).
5. If floating particulates remained, the solution was centrifuged (Hermle Z383K, 2500 rpm, 5 min).

The dilution factors were selected on expected elemental concentrations, guided by XRF composition of sample F (32025006 009, milled magnetic slag). From each 50 mL digest, dilutions were prepared, including a 100× dilution (0.1 mL → 10 mL), typically yielding appropriate concentrations within the ICP TQ calibration range (1–200 µg/L).

Elemental analysis was performed using an Agilent 8900 ICP-TQ with:

- SPS4 autosampler
- Quartz torch and spray chamber
- MicroMist quartz nebulizer
- Nickel cones with X-lens
- MassHunter 5.2 for quantification

Ion modes applied included NoGas, He, H_2, and O_2 depending on the sample. Results were converted to mg/kg (ppm) of original material using all dilution and phase fraction corrections.

4.5 XRF Analysis

For comparison with ICP-MS results, samples F and R were analyzed by x-ray fluorescence spectroscopy (XRF) using a Bruker S2 PUMA. The samples were used as received and approximately 7 g was loaded into XRF cups. Quantification used the SMART Oxides calibration to report oxide concentrations (wt%).

5 Results and discussion

Table 2 shows the concentrations of different elements (in wt.%) resulting from ICP-MS measurements. The colours show the magnitude of concentration for a sample in comparison with the other samples (darker green and red mean relatively high in solid and liquid samples respectively). Solid and liquid samples are compared separately since the solid samples overall show significantly higher concentration of CRMs.

Among the liquid samples, only samples A and B showed higher concentrations; however, the values were still around an order of magnitude lower than the solids. The increased concentrations can be explained by the presence of fines from the sludge that do contain CRMs. It may be concluded that no CRMs are dissolved in the washing steps.

5.1 Outlier data points

All table entries are based upon a single measurement of 0.1 grams, therefore, extreme outlier data points (marked in yellow) should be viewed with caution. Outlier data points are values that fall outside the typical spread of the data, specifically those that lie below the first quartile (Q1) minus 1.5 times the interquartile range (IQR) or above the third quartile (Q3) plus 1.5 times the IQR. The first quartile (Q1) marks the 25th percentile of the data, while the IQR represents the middle 50% of values (Q3 – Q1), making any points beyond this 1.5×IQR boundary unusually distant from the central distribution.

For instance, sample R which is a coarse-particle sample coming from a separation step in WASI 2, shows a significantly high copper and nickel concentration, 25 and 0.41 wt.%, respectively. These are the highest Cu and Ni concentrations among all samples. This is most likely due to limitations in sampling coarse particles. It is possible that a more compositionally pure particle containing Cu and Ni was sampled by chance. The absence of Mg in this sample further suggests that it may not be representative.

		Sample code	Concentration of elements (wt.%)										
			B	Mg	Al	P	Ti	Mn	Co	Ni	Cu	Sr	Ba
Solid samples		F	0.0065	0	3.42	0.19	0.13	0.0347	0	0.0073	0.15	0.0139	0.0563
		F	0.0097	0	1.45	0.16	0.14	0.0357	0	0.0063	0.29	0.0148	0.068
		G	0.0069	0	1.26	0.22	0.17	0.0806	0.0029	0.0095	0.35	0.0192	0.0732
		H	0.011	0.56	1.54	0.31	0.23	0.12	0.0032	0.0113	0.3	0.0242	0.12
		I	0	0	0.93	0.1	0.0974	0.0229	0	0	0.16	0.0107	0.0319
		J	0	0	1.24	0.15	0.0857	0.0457	0	0	0.16	0.0097	0.0373
		K	0.0056	0	1.59	0.19	0.16	0.0673	0.0027	0.0095	0.32	0.0163	0.0532
		L	0.0051	0	1.48	0.19	0.14	0.0875	0	0.0106	0.98	0.0156	0.0619
		M	0.0225	0.6	2.1	0.32	0.43	0.16	0.0053	0.0435	0.37	0.0342	0.17
		M	0.0224	0.62	2.18	0.32	0.42	0.15	0.0078	0.0314	0.3	0.0346	0.16
		N	0.0138	0.55	2.16	0.27	0.33	0.52	0.0073	0.0544	7.64	0.0306	0.15
		O	0.0156	0.58	2.07	0.31	0.3	0.0591	0.0044	0.0156	0.18	0.0271	0.12
		P	0.0137	0.58	2.28	0.35	0.29	0.1	0.0079	0.026	0.33	0.0276	0.11
		Q	0.0176	0.56	1.64	0.29	0.29	0.061	0.0029	0.0116	0.6	0.0262	0.11
		R	0.0142	0	1.72	0.18	0.35	0.23	0.0036	0.4093	25.12	0.0288	0.14
		S	0.0131	0.52	2.29	0.19	0.26	0.0909	0	0.0116	0.37	0.0235	0.11
		T	0.0148	0.54	2.23	0.28	0.32	0.11	0.0056	0.0201	0.24	0.0277	0.12
		U	0.0165	0.56	1.98	0.23	0.3	0.0857	0.0026	0.0132	0.25	0.0251	0.11
		V	0.0142	0.74	2.09	0.37	0.31	0.0961	0.007	0.0215	0.29	0.0325	0.13
		V	0.0129	0.71	2.04	0.36	0.28	0.1	0.0646	0.0273	0.83	0.0326	0.11
		W	0.018	0.67	1.89	0.31	0.34	0.12	0.0094	0.0488	0.49	0.0367	0.14
		X	0.0162	0.55	1.82	0.28	0.28	0.0652	0.0038	0.0199	0.29	0.0292	0.11
		Y	0.0148	0.74	2.61	0.39	0.3	0.0921	0.0081	0.0284	0.35	0.0358	0.14
		Z	0.0165	0.71	2.31	0.4	0.3	0.084	0.007	0.0225	0.29	0.0377	0.15
		AA	0.0136	0.58	2.09	0.3	0.31	0.26	0.0171	0.0609	0.5	0.0342	0.13
		AB	0.0165	0.52	1.79	0.25	0.33	0.1	0.0035	0.0227	0.22	0.0268	0.12
		AB	0.0166	0.52	1.74	0.26	0.35	0.1	0.0028	0.0226	0.24	0.0273	0.12
		AC	0	0	0.7	0.12	0.0618	0.0223	0	0	0.16	0.017	0.038
		AD	0.0095	1.01	2.66	0.41	0.33	0.0887	0.0071	0.0241	0.37	0.0455	0.14
		AE	0.0177	0.53	1.79	0.31	0.22	0.0475	0.0039	0.0109	0.17	0.0239	0.0966
		AF	0.0108	0.61	2.83	0.35	0.29	0.12	0.0107	0.0299	0.33	0.0298	0.11
The concentrations for solid and liquid samples (above and below this blue line) are compared separately													
Liquid samples	Filtered liquid	A	0.0002	0.005	0.0001	4E-05	2E-05	1E-05	0	2E-05	1E-05	0.0006	3E-05
		B	0.0002	0.0035	6E-05	2E-05	2E-05	0	0	2E-05	1E-05	0.0006	2E-05
		C	0.0002	0.0146	5E-05	1E-05	1E-05	0	0	1E-05	0	0.0004	2E-05
		D	7E-05	0.0043	4E-05	0	0	1E-05	0	0	1E-05	0.0001	1E-05
		E	0.0001	0.0035	0.0003	2E-05	1E-05	2E-05	0	1E-05	0.0001	0.0002	1E-05
	Residu	A	0.0014	0.1379	0.3394	0.0498	0.0407	0.0103	0.0007	0.0028	0.0487	0.0056	0.0189
		B	0.0021	0.1627	0.4358	0.0704	0.052	0.0138	0.0014	0.0042	0.0546	0.0073	0.0251
		C	0	0.0005	0.0004	0.0002	5E-05	2E-05	0	1E-05	0.0002	0	0.0001
		D	0	0.0008	0.003	0.0003	0.0003	4E-05	1E-05	2E-05	0.0005	0	0.0001
		E	0.0001	0.0128	0.0387	0.0054	0.0041	0.0015	0.0001	0.0004	0.0064	0.0006	0.002
	Liquid +Residu	A	0.0016	0.14	0.34	0.0499	0.0407	0.0103	0.0008	0.0028	0.0488	0.0062	0.019
		B	0.0023	0.17	0.44	0.0704	0.0521	0.0138	0.0014	0.0042	0.0546	0.0079	0.0252
		C	0.0002	0.0151	0	0	7E-05	0	0	0	0.0002	0.0005	8E-05
		D	7E-05	0.0051	0.0031	0	0.0003	0	0	0	0.0005	0.0001	0.0001
		E	0.0003	0.0163	0.039	0.0054	0.0041	0.0015	0.0001	0.0004	0.0066	0.0008	0.0021

Table 2: The concentration of main elements in the samples taken from different stages of bottom ash processing. The yellow cells are removed from the colour ranking as outliers. The four darker grey measurements (samples F, M, V, AB) are duplo measurements.

5.2 XRF cross examination

To verify this potential outlier, a cross examination by XRF measurements was performed on a sample showing an outlier, sample R, and a sample containing an average concentration of CRMs, sample F. Table 3 and 4 present both the XRF and ICP-MS measurements for iron, aluminum, copper and titanium for both samples. The elemental concentrations were calculated by converting the oxide data to elemental concentrations using the molecular mass.

Oxide/Element	Oxide - XRF	Element - XRF	Element - ICP MS
Fe_2O_3/Fe	2.07	1.45	1.04
Al_2O_3/Al	9.54	5.05	3.42
CuO/Cu	0.21	0.17	0.15
TiO_2/Ti	0.63	0.38	0.13

Table 4: A comparison for sample F between weight percentages as a result from XRF and ICP-MS.

Oxide/Element	Oxide - XRF	Element - XRF	Element - ICP MS
Fe_2O_3/Fe	16.18	1.13	10.34
Al_2O_3/Al	46.44	2.46	1.72
CuO/Cu	0.44	0.35	25.12
TiO_2/Ti	0.38	0.23	0.35

Table 3: A comparison for sample R between weight percentages as a result from XRF and ICP-MS.

The XRF results for the non-ferrous sample F are similar to the ICP-MS data point. The data of the coarse concentrate sample R however differs substantially. This is probably due to the coarse nature of sample R and the small ICP-MS sample size. As suspected earlier, the used ICP-MS sample scoop could have contained more milled copper (for instance from a copper wire) and less aluminum by accident. Given this outcome, it was decided to discard the ICP-MS datapoint for sample R and sample N probably too. But then again, the reported XRF results are also the outcome of a single measurement on a relatively small sample weight.

This study presents a first assessment of CRM-concentrations. Additional measurements are needed to confirm actual CRM-concentrations with relative certainty, which is further discussed in chapter 6.

Another outlier value is seen for the fine-particle sample N coming from the same separation step in WASI 2. This sample shows the second highest copper concentration of 7.64 wt.% and highest Mn concentration of 0.52 wt.%. While samples R and N show promising values for CRMs, it should be noted that such results can be due to errors in sampling or the ICP measurements.

5.3 General outcomes

In addition, although it is not possible to provide precise insight into the elemental composition of individual samples, some general trends can still be observed. For the non-ferro samples F-L, generally lower concentrations were measured compared with M-AF. This may be explained by the fact that samples F-L are non-ferrous samples which contain about 70-80% coarse (non-ferro) metallic particles (see Supplementary material). The coarse metallic particles have been separated from the materials that have been measured. As such, the data reported here only represent a small fraction of the sample, possibly resulting in a large fraction of the (CRM-) metals within these materials streams is not measured in this study and are not reflected in the current data set. Given the metallic nature of these separated materials, these would probably increase the final concentration of several CRMs, but this remains to be researched.

The ferrous and non-ferrous metallic fractions for samples M-AA was in the range of 1-9 wt%. The CRM concentrations reported in Table 2 are therefore up to 10 % lower in the original material streams. Other samples that show similarities in composition are the materials coming from the magnetic slag material streams, samples M, W and AA. The measurement data only shows a relatively higher concentration of Ni. Samples V, X, Y, and Z are all separated based on similar physical properties in different steps, yielding material streams with similar composition.

Sample AC shows almost no presence of CRMs which is resulting from the fact that this is organic gravel and mostly consist of small wood chips and plastics.

Although there are certainly differences in composition, it is difficult to pinpoint a specific material stream with a significantly higher concentration of CRMs, but many of the samples show the presence of CRMs such as Cu, Ni, Al, Sr, Mn, Ti, P, Mg and B.

5.4 CRM data distribution

Figure 6 presents the distribution of elemental concentrations measured across all samples. Each data point is shown as a small circle aligned vertically for the corresponding element, with each circle representing one sample measurement. For example, for Al, all values listed in the Al column of Table 2 are plotted here. The figure indicates that Al concentrations range from a minimum of 0.7 wt.% (sample AC) to a maximum of approximately 3.5 wt.% (sample F). The central box in each plot represents the interquartile range (IQR), capturing the middle 50% of the data, while the horizontal line within the box denotes the median concentration. The whiskers extend to the minimum and maximum values excluding outliers.

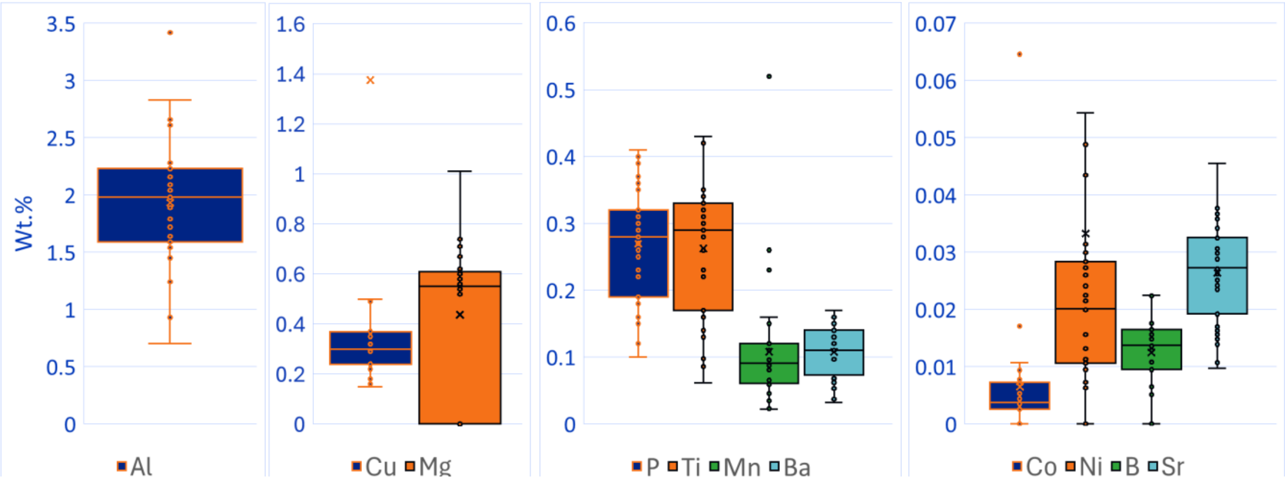

Figure 6: The distribution of concentration values (in wt.%) of samples for different elements. The previously mentioned outlier data points are removed from this picture for copper (2 top) and nickel (1 top).

Major outliers previously identified for Cu and Ni were removed prior to plotting and are therefore not shown. Because concentration ranges differ substantially among elements, the elements are grouped into separate graphs, each with its own Y-axis scale to ensure clarity. Elements that are not included in these panels exhibited negligible concentrations and are instead reported in the Supplement Data.

5.5 Literature comparison

To compare the measured values with theoretical expectations, the average composition of the solid samples is evaluated and compared with two previous studies (Hjelmar 2013 and Dijkstra 2019) in Figure 7. The results show that most element concentrations align with earlier findings on various bottom ashes, indicating that although minor differences exist between ashes from different sources, their overall composition remains broadly similar. Notable deviations are observed for Al, Mg, P, and Ti, for which our study reports lower average values compared with the previously published data.

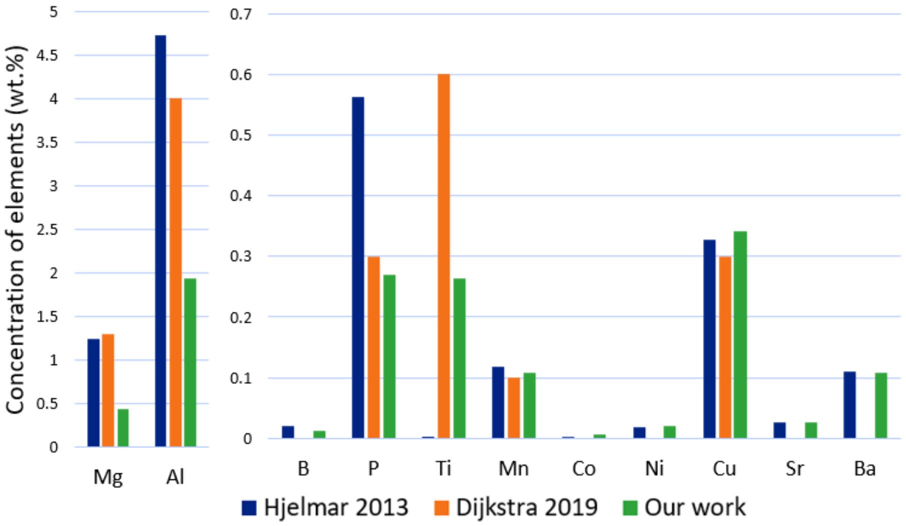

Figure 7: Average elemental composition (in wt.%) of bottom ash used in our work compared with values from works by Hjelmar 2013 and Dijkstra 2019.

In order to make the concentration values more understandable, they are compared with the mining grade range from their ore. For example, more than 80% of the world's identified copper resources occur in porphyry and sediment-hosted deposits. Porphyry copper deposits are large-scale, low-grade ore bodies typically containing 0.2% to over 1% copper (Singer, 2017). Therefore, it can be concluded that most of the measured bottom ash samples have a copper concentration comparable to the mined copper ores. Comparing the measured concentration values with the mining grades for different elements, it is found that there are samples with Co, Cu and Sr concentrations in the same range as some mining grades (green highlighted cells in table 5 below).

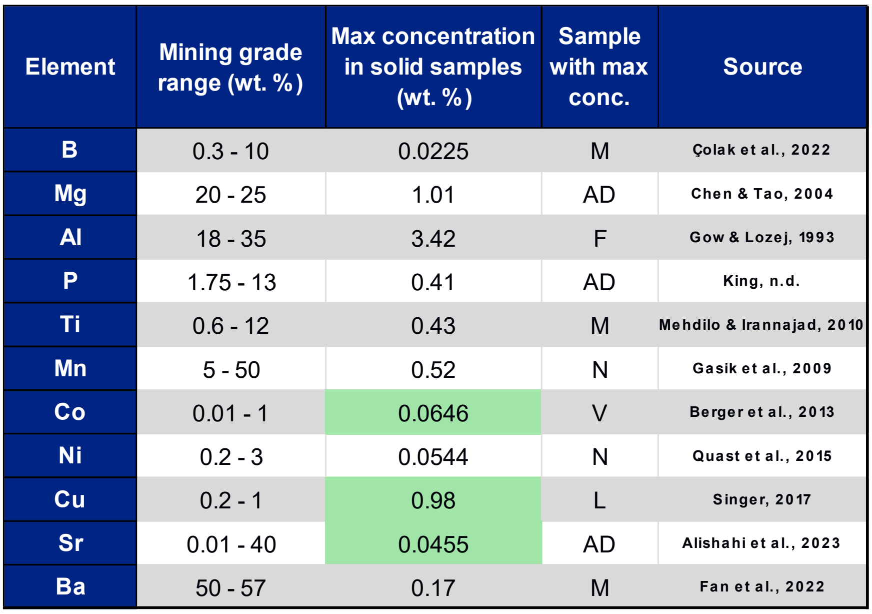

Element	Mining grade range (wt. %)	Max concentration in solid samples (wt. %)	Sample with max conc.	Source
B	0.3 - 10	0.0225	M	Çolak et al., 2022
Mg	20 - 25	1.01	AD	Chen & Tao, 2004
Al	18 - 35	3.42	F	Gow & Lozej, 1993
P	1.75 - 13	0.41	AD	King, n.d.
Ti	0.6 - 12	0.43	M	Mehdilo & Irannajad, 2010
Mn	5 - 50	0.52	N	Gasik et al., 2009
Co	0.01 - 1	0.0646	V	Berger et al., 2013
Ni	0.2 - 3	0.0544	N	Quast et al., 2015
Cu	0.2 - 1	0.98	L	Singer, 2017
Sr	0.01 - 40	0.0455	AD	Alishahi et al., 2023
Ba	50 - 57	0.17	M	Fan et al., 2022

Table 5. The maximum concentration of elements in solid samples compared with the mining grade range of them, both in wt.%. Green cells show the values that fall in the mining grade range. The outlier values are not considered here (two top values of copper and one for nickel).

6 Conclusion

This research provides insight into the availability and dilution of critical raw materials from bottom ash treatment material streams. The ICP-MS results indicate a presence of a spectrum of CRMs across all material streams. Under the limited sample assessment, some samples show concentrations similar to ore grades for Cu, Co and Sr. It appears that the concentration of CRMs is rather homogenous, and thus that the array of mechanical sorting techniques has a limited effect on CRM concentrations. Therefore, the hypothesis that the treatment processes locally increase CRM concentrations in certain material streams under the assessed conditions cannot be confirmed.

However, it should be noted that the results reported in this report are based on a single ICP-MS measurement on a small sample. Given the heterogeneous nature of bottom ash, there is a large chance that our measurements do not reflect the overall composition of the material streams, but only the analyzed ICP-MS sample scoop. Therefore, more data points are needed to verify the reported results, as also marked in the next section on follow-up research.

6.1 Follow up research

The NMO has provided a first step to support in analyzing the CRM concentrations of bottom ash treatment material streams. Several additional research activities are required to verify our explorative results and potentially recover CRMs once their presence is confirmed. As such, other parties are needed to take the lead in these follow-up activities that fall outside the scope of the NMO.

6.1.1 Additional analysis

A next step in mining this potential would be to verify the current results by additional analysis. As stated before, all results originated from a single ICP-MS measurement on a single sample of typically 0.1 g. Additional measurements should validate the presence and concentration of CRMs.
Preferably, the coarse fraction of samples would also be analyzed. This could require heavy milling or even melting the coarse (ferrous) parts within samples.

6.1.2 Recycling process analysis

In addition to sample analysis, an effect analysis on the recycling route could also be performed. By looking at the differences in concentration between samples taken before and after certain recycling steps, we quantify the actual effect of these recycling measures. This information could potentially prove valuable in increasing the concentration (and thus potential recovery) of CRMs.

6.1.3 Hydrometallurgy research

The actual recovery of certain CRMs could be researched in parallel. Given the polluted and diluted nature of the material streams, hydrometallurgical processing seems the most probable route for recovery. We recommend exploring specialized metallurgical methods for recovery of specific CRMs, more specifically the quantity and quality of recovered materials.

6.1.4 Bottom ash from other origins

Finally, this research scope could be widened to other bottom ash batches, and also samples from bottom ash washers in the Netherlands or abroad. Given that bottom ash reflects the input waste, other bottom ash samples could point to higher CRMs concentrations. Heros points out for example that French bottom ash generally contains more metals than Dutch bottom ash. In addition, bottom ashes from specialized industrial or hospital waste incineration could be assessed.

A.1 Supplement data

Weight of samples and removed coarse fractions

Table 6 lists the weights of the received samples and the percentage of coarse particles within that have been removed.

	Weight in gram					
Sample code	**Sample 0-2mm bulk**	**Sample 0-2mm milled**	**Removed coarse (>2mm)**	**Removed coarse non-ferrous (>2mm)**	**Total sample weight**	**%Removed coarse fraction**
F	486.01	122.01	170.58	1634.4	2413.00	75%
G	412.38	112.39	291.95	1177.0	1993.72	74%
H	322.51	130.87	234.73	841.0	1529.11	70%
I	406.73	123.91	300.91	2651.2	3482.75	85%
J	444.99	113.01	466.57	2415.5	3440.07	84%
K	433.69	88.14	390.92	1804.7	2717.45	81%
L	408.00	112.69	292.73	970.0	1783.42	71%
M	3141.9	121.87	69.15		3332.92	2%
N	2756.1	130.20	250.40		3136.70	8%
O	2011.1	131.92	110.97		2253.99	5%
P	2054.8	137.00	23.16		2214.96	1%
Q	1711.4	138.31	78.37		1928.08	4%
R	3346.9	130.49	335.37		3812.76	9%
S	2459.4	128.58	94.47		2682.45	4%
T	2326.3	120.90	59.57		2506.77	2%
U	3024.0	125.77	104.00		3253.77	3%
V	2124.3	114.73	31.20		2270.23	1%
W	2841.2	105.43	90.99		3037.62	3%
X	2474.2	132.39	132.97		2739.56	5%
Y	1774.4	104.97	88.24		1967.61	4%
Z	1751.1	95.21	114.05		1960.36	6%
AA	2098.5	112.72	77.70		2288.92	3%
AB	278.46	381.54	306.68		966.68	32%
AC	158.88	114.63	348.05		621.56	56%
AD	147.92	87.87	86.03		321.82	27%
AE	115.2	158.66	180.05		453.91	40%
AF	206.55	245.35	58.16		510.06	11%

Table 6: Weight of samples and removed fractions.

Weigh percentage solid residue in liquid samples

Table 7 reports the weight percentage of the solid residue in liquid samples.

Sample code	Dry weight percentage solid residue
A	11.70%
B	16.40%
C	0.27%
D	0.06%
E	1.20%

Table 7: Dry weight percentages of the solid residue in liquid samples.

Results sample analysis

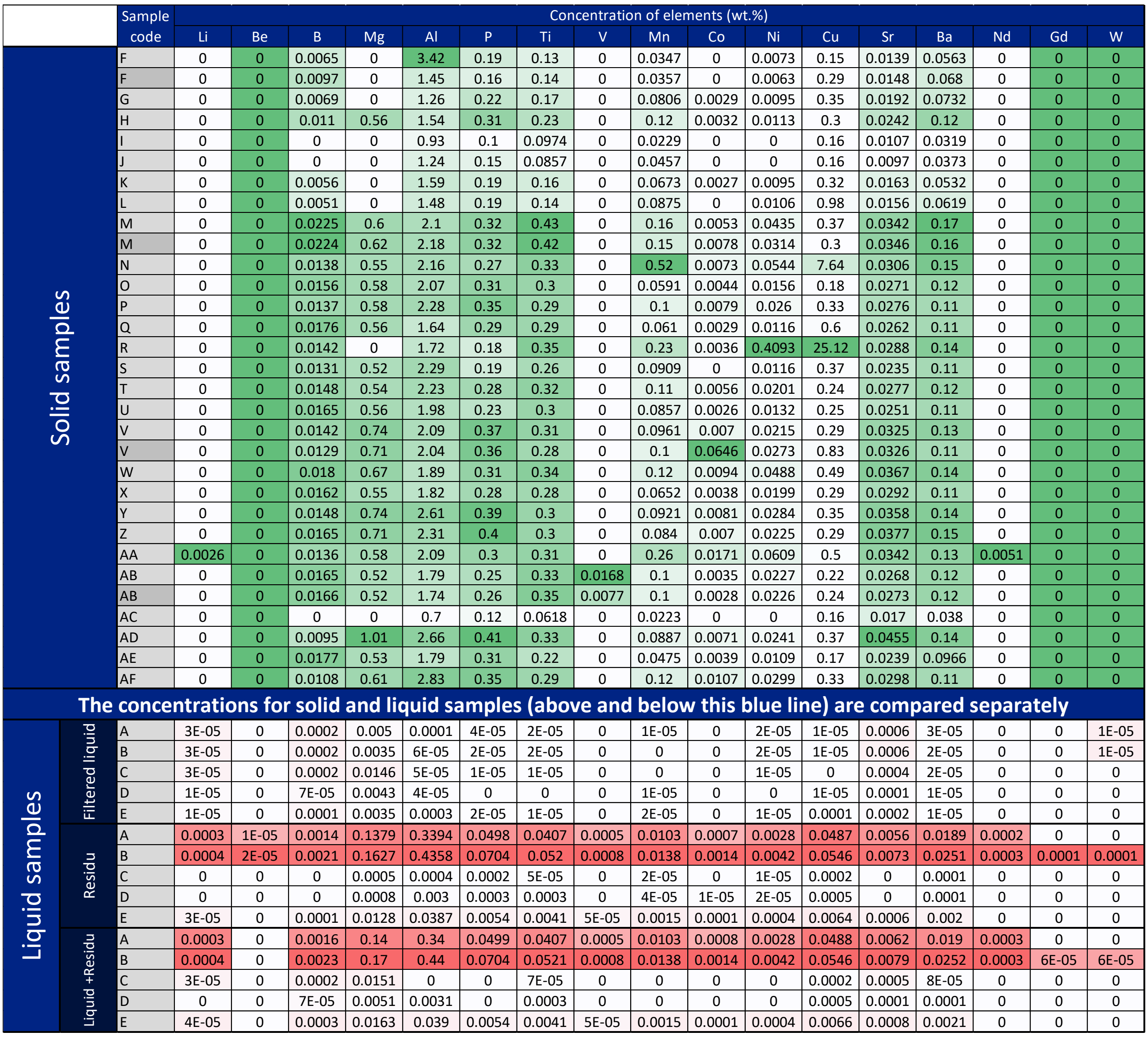

		Sample code	Concentration of elements (wt.%)															
			Li	Be	B	Mg	Al	P	Ti	V	Mn	Co	Ni	Cu	Sr	Ba	Nd	Gd	W
Solid samples		F	0	0	0.0065	0	3.42	0.19	0.13	0	0.0347	0	0.0073	0.15	0.0139	0.0563	0	0	0
		F	0	0	0.0097	0	1.45	0.16	0.14	0	0.0357	0	0.0063	0.29	0.0148	0.068	0	0	0
		G	0	0	0.0069	0	1.26	0.22	0.17	0	0.0806	0.0029	0.0095	0.35	0.0192	0.0732	0	0	0
		H	0	0	0.011	0.56	1.54	0.31	0.23	0	0.12	0.0032	0.0113	0.3	0.0242	0.12	0	0	0
		I	0	0	0	0	0.93	0.1	0.0974	0	0.0229	0	0	0.16	0.0107	0.0319	0	0	0
		J	0	0	0	0	1.24	0.15	0.0857	0	0.0457	0	0	0.16	0.0097	0.0373	0	0	0
		K	0	0	0.0056	0	1.59	0.19	0.16	0	0.0673	0.0027	0.0095	0.32	0.0163	0.0532	0	0	0
		L	0	0	0.0051	0	1.48	0.19	0.14	0	0.0875	0	0.0106	0.98	0.0156	0.0619	0	0	0
		M	0	0	0.0225	0.6	2.1	0.32	0.43	0	0.16	0.0053	0.0435	0.37	0.0342	0.17	0	0	0
		M	0	0	0.0224	0.62	2.18	0.32	0.42	0	0.15	0.0078	0.0314	0.3	0.0346	0.16	0	0	0
		N	0	0	0.0138	0.55	2.16	0.27	0.33	0	0.52	0.0073	0.0544	7.64	0.0306	0.15	0	0	0
		O	0	0	0.0156	0.58	2.07	0.31	0.3	0	0.0591	0.0044	0.0156	0.18	0.0271	0.12	0	0	0
		P	0	0	0.0137	0.58	2.28	0.35	0.29	0	0.1	0.0079	0.026	0.33	0.0276	0.11	0	0	0
		Q	0	0	0.0176	0.56	1.64	0.29	0.29	0	0.061	0.0029	0.0116	0.6	0.0262	0.11	0	0	0
		R	0	0	0.0142	0	1.72	0.18	0.35	0	0.23	0.0036	0.4093	25.12	0.0288	0.14	0	0	0
		S	0	0	0.0131	0.52	2.29	0.19	0.26	0	0.0909	0	0.0116	0.37	0.0235	0.11	0	0	0
		T	0	0	0.0148	0.54	2.23	0.28	0.32	0	0.11	0.0056	0.0201	0.24	0.0277	0.12	0	0	0
		U	0	0	0.0165	0.56	1.98	0.23	0.3	0	0.0857	0.0026	0.0132	0.25	0.0251	0.11	0	0	0
		V	0	0	0.0142	0.74	2.09	0.37	0.31	0	0.0961	0.007	0.0215	0.29	0.0325	0.13	0	0	0
		V	0	0	0.0129	0.71	2.04	0.36	0.28	0	0.1	0.0646	0.0273	0.83	0.0326	0.11	0	0	0
		W	0	0	0.018	0.67	1.89	0.31	0.34	0	0.12	0.0094	0.0488	0.49	0.0367	0.14	0	0	0
		X	0	0	0.0162	0.55	1.82	0.28	0.28	0	0.0652	0.0038	0.0199	0.29	0.0292	0.11	0	0	0
		Y	0	0	0.0148	0.74	2.61	0.39	0.3	0	0.0921	0.0081	0.0284	0.35	0.0358	0.14	0	0	0
		Z	0	0	0.0165	0.71	2.31	0.4	0.3	0	0.084	0.007	0.0225	0.29	0.0377	0.15	0	0	0
		AA	0.0026	0	0.0136	0.58	2.09	0.3	0.31	0	0.26	0.0171	0.0609	0.5	0.0342	0.13	0.0051	0	0
		AB	0	0	0.0165	0.52	1.79	0.25	0.33	0.0168	0.1	0.0035	0.0227	0.22	0.0268	0.12	0	0	0
		AB	0	0	0.0166	0.52	1.74	0.26	0.35	0.0077	0.1	0.0028	0.0226	0.24	0.0273	0.12	0	0	0
		AC	0	0	0	0	0.7	0.12	0.0618	0	0.0223	0	0	0.16	0.017	0.038	0	0	0
		AD	0	0	0.0095	1.01	2.66	0.41	0.33	0	0.0887	0.0071	0.0241	0.37	0.0455	0.14	0	0	0
		AE	0	0	0.0177	0.53	1.79	0.31	0.22	0	0.0475	0.0039	0.0109	0.17	0.0239	0.0966	0	0	0
		AF	0	0	0.0108	0.61	2.83	0.35	0.29	0	0.12	0.0107	0.0299	0.33	0.0298	0.11	0	0	0
The concentrations for solid and liquid samples (above and below this blue line) are compared separately																		
Liquid samples	Filtered liquid	A	3E-05	0	0.0002	0.005	0.0001	4E-05	2E-05	0	1E-05	0	2E-05	1E-05	0.0006	3E-05	0	0	1E-05
		B	3E-05	0	0.0002	0.0035	6E-05	2E-05	2E-05	0	0	0	2E-05	1E-05	0.0006	2E-05	0	0	1E-05
		C	3E-05	0	0.0002	0.0146	5E-05	1E-05	1E-05	0	0	0	1E-05	0	0.0004	2E-05	0	0	0
		D	1E-05	0	7E-05	0.0043	4E-05	0	0	0	1E-05	0	0	1E-05	0.0001	1E-05	0	0	0
		E	1E-05	0	0.0001	0.0035	0.0003	2E-05	1E-05	0	2E-05	0	1E-05	0.0001	0.0002	1E-05	0	0	0
	Residu	A	0.0003	1E-05	0.0014	0.1379	0.3394	0.0498	0.0407	0.0005	0.0103	0.0007	0.0028	0.0487	0.0056	0.0189	0.0002	0	0
		B	0.0004	2E-05	0.0021	0.1627	0.4358	0.0704	0.052	0.0008	0.0138	0.0014	0.0042	0.0546	0.0073	0.0251	0.0003	0.0001	0.0001
		C	0	0	0	0.0005	0.0004	0.0002	5E-05	0	2E-05	0	1E-05	0.0002	0	0.0001	0	0	0
		D	0	0	0	0.0008	0.003	0.0003	0.0003	0	4E-05	1E-05	2E-05	0.0005	0	0.0001	0	0	0
		E	3E-05	0	0.0001	0.0128	0.0387	0.0054	0.0041	5E-05	0.0015	0.0001	0.0004	0.0064	0.0006	0.002	0	0	0
	Liquid +Residu	A	0.0003	0	0.0016	0.14	0.34	0.0499	0.0407	0.0005	0.0103	0.0008	0.0028	0.0488	0.0062	0.019	0.0003	0	0
		B	0.0004	0	0.0023	0.17	0.44	0.0704	0.0521	0.0008	0.0138	0.0014	0.0042	0.0546	0.0079	0.0252	0.0003	6E-05	6E-05
		C	3E-05	0	0.0002	0.0151	0	0	7E-05	0	0	0	0	0.0002	0.0005	8E-05	0	0	0
		D	0	0	7E-05	0.0051	0.0031	0	0.0003	0	0	0	0	0.0005	0.0001	0.0001	0	0	0
		E	4E-05	0	0.0003	0.0163	0.039	0.0054	0.0041	5E-05	0.0015	0.0001	0.0004	0.0066	0.0008	0.0021	0	0	0

Table 8: The ICP-MS data set for all CRMs, including the (near) zero value elements.

References

Alishahi, A., Noaparast, M., Ashni, A. R., & Nasab, M. H. (2023). The optimization of the strontium compounds production, using a celestine ore sample. Rudarsko-geološko-naftni zbornik, 38(4), 53-62.

Astrup, T., Muntoni, A., Polettini, A., Pomi, R., Van Gerven, T., Van Zomeren, A., 2016. Treatment and reuse of incineration bottom ash. Environmental Materials and Waste Resource Recovery and Pollution Prevention. https://doi.org/10.1016/B978-0-12-803837-6.00024-X.

Berger, T., Walker, R., & Johnson, M. (2013). *Effect of solution chemistry on magnesite/dolomite flotation* International Journal of Mineral Processing, 118, 18–29. https://doi.org/10.1016/j.minpro.2013.01.014

Chen, G., & Tao, D. (2004). Effect of solution chemistry on flotability of magnesite and dolomite. International Journal of Mineral Processing, 74(1-4), 343-357.

Çolak, A., Laratte, B., Elevli, B., & Çoruh, S. (2022). Abiotic depletion of boron: an update characterization factors for CML 2002 and ReCiPe. Minerals, 12(4), 435.

Dijkstra et al. (2019) The geological significance of novel anthropogenic materials : Deposits of industrial waste and by-products. Anthropocene, 28, 100229 http://dx.doi.org/10.1016/j.ancene.2019.100229

European Parliament and the Council of the European Union. (2024). Regulation (EU) 2024/1157 of the European Parliament and of the Council of 11 April 2024 on shipments of waste, amending Regulations (EU) No 1257/2013 and (EU) 2020/1056 and repealing Regulation (EC) No 1013/2006. 145. https://eur-lex.europa.eu/legal-content/EN/TXT/PDF/?uri=OJ:L_202401157

Funari et al (2015)., Solid residues from Italian municipal solid waste incinerators: A source for “critical” raw materials. https://www.sciencedirect.com/science/article/pii/S0956053X14005212?via%3Dihub

Gasik, M. I., Gladkikh, V. A., Zhdanov, A. V., Zhuchkov, V. I., Zayakin, O. V., Leont’ev, L. I., & Ovcharuk, A. N. (2009). *Calculation of the value of manganese ore raw materials*. Russian Metallurgy (Metally, 2009(8)), 756–758. https://doi.org/10.1134/

Ghani et al (2023)., Impact and recoverability of metals from waste: a case study on bottom ash from municipal solid waste incineration plants. https://www.frontiersin.org/journals/environmental-science/articles/10.3389/fenvs.2023.1252313/full

Gow, N. N., & Lozej, G. P. (1993). Bauxite. Geoscience Canada, 20(1), 9-16.

Heros, personal communication

Hjelmar et al (2013)., HP classification of European incinerator bottom ash. Part 1: Compilation of data on IBA composition and leaching properties. Part 2: Assessment of hazardous properties of IBA; 2013

King, H. M. (n.d.). *Apatite, phosphorite and phosphate rock*. Retrieved January 23, 2026, from https://www.erudit.org/en/journals/geocan/1993-v20-n1-geocan_20_1/geocan20_1art02.pdf

Mehdilo, A., & Irannajad, M. (2010). *Applied mineralogical studies on Iranian hard rock titanium deposit*. Journal of Minerals and Materials Characterization and Engineering, 9(3), 247–262. Retrieved January 23, 2026, from https://www.scirp.org/pdf/JMMCE20100300006_32990359.pdf

Quast, K., Connor, J. N., Skinner, W., Robinson, D. J., & Addai-Mensah, J. (2015).

Preconcentration strategies in the processing of nickel laterite ores Part 1: Literature review. Minerals Engineering, 79, 261-268.

Singer, D. A. (2017). Future copper resources. Ore Geology Reviews, 86, 271-279.

Syc et al (2020)., Metal recovery from incineration bottom ash: State-of-the-art and recent developments. Journal of Hazardous Materials, 393, 122433

TNO (2025)., Critical Raw Materials Potential in the Netherlands' Subsurface.
van Geffen, P.W.G., Lips, A.L.W., Raat, H.A., Stam, J.C., Versluis, F.C., Wasch, L.J.

TNO (2026)., The state of play of the Dutch recycling industry *(to be published).*
Campbell – Johnston, K.A., Jung, H., Huitema, D.M.M., Kamps, M.T., Lennartz, J., Vera Concha, I.C.

Netherlands Materials Observatory

Princetonlaan 6
3584 CB Utrecht
www.nederlandsmaterialenobservatorium.nl/en/

TNO

Nederlands
Materialen
Observatorium